Biophysical Journal Volume 92 June 2007 3949–3959

Biphenyl Bicelle Disks Align Perpendicular to Magnetic Fields on Large Temperature Scales: A Study Combining Synthesis, Solid-State NMR, TEM, and SAXS

Cécile Loudet,* Sabine Manet,* Stéphane Gineste,† Reïko Oda,* Marie-France Achard,† and Erick J. Dufourc*

*UMR 5248 CBMN, CNRS-Université Bordeaux 1-ENITAB, Institut Européen de Chimie et Biologie, Pessac, France; and †UPR 8641, Centre de Recherche Paul Pascal, CNRS, Pessac, France

ABSTRACT A phosphatidylcholine lipid (PC) containing a biphenyl group in one of its acyl chains (1-tetradecanoyl-2-(4-(4-biphenyl)butanoyl)-*sn*-glycero-3-PC, TBBPC) was successfully synthesized with high yield. Water mixtures of TBBPC with a short-chain C_6 lipid, dicaproyl-PC (DCPC), lead to bicelle systems formation. Freeze-fracture electron microscopy evidenced the presence of flat bilayered disks of 800 Å diameter for adequate composition, hydration, and temperature conditions. Because of the presence of the biphenyl group, which confers to the molecule a positive magnetic anisotropy $\Delta\chi$, the disks align with their normal, n, parallel to the magnetic field B_0, as directly detected by ^{31}P, ^{14}N, ^{2}H solid-state NMR and also using small-angle x-ray scattering after annealing in the field. Temperature-composition and temperature-hydration diagrams were established. Domains where disks of TBBPC/DCPC align with their normal parallel to the field were compared to chain-saturated lipid bicelles made of DMPC(dimyristoylPC)/DCPC, which orient with their normal perpendicular to B_0. TBBPC/DCPC bicelles exist on a narrow range of long- versus short-chain lipid ratios (3%) but over a large temperature span around room temperature (10–75°C), whereas DMPC/DCPC bicelles exhibit the reverse situation, i.e., large compositional range (22%) and narrow temperature span (25–45°C). The two types of bicelles present orienting properties up to 95% dilution but with the peculiarity that water trapped in biphenyl bicelles exhibits ordering properties twice as large as those observed in the saturated-chains analog, which offers very interesting properties for structural studies on hydrophilic or hydrophobic embedded biomolecules.

INTRODUCTION

Understanding the function of proteins is tightly linked to the determination of protein atomic structure and dynamics. In studying membrane proteins, finding the topology/orientation at or in the membrane lipid bilayer is also of first importance. Among all spectroscopic techniques leading to such information, NMR, both in its solution and solid-state versions, is a powerful technique to study proteins in a membrane environment (1–3). Several innovative models of biological membranes such as micelles (4,5) and multilamellar (6) or unilamellar (7) vesicles were thus customized to investigate structure and dynamics of integral membrane proteins having single or multiple transmembrane segments (8). To improve the spectral NMR resolution and particularly to determine the orientation of membrane proteins, it is interesting to orient these models in a magnetic field, B_0. Membrane systems sandwiched between glass plates that are macroscopically oriented in the magnetic field are tested, but a difficult control of the sample hydration limits their use (9,10). Since the mid 1980s, a new membrane model, called a ''bicelle,'' has become very popular (11,12) because it orients spontaneously in magnetic fields and because both magic angle spinning and wide-line NMR experiments may be performed with the same well-hydrated sample (13,14). Bicelles represent an intermediate model membrane between lipid vesicles and classical micelles. They are composed of mixtures of long-chain phospholipids (14–18 carbons) and short-chain phospholipids (6–8 carbons) and may take several morphologies depending on composition (X = [long chain]/[total lipid]), temperature, and hydration (h = water mass/total mass). Disk-shaped, cylindrical ''wormlike'' micelles and perforated lamellae have been reported (15–22). Disk dimensions of 30–60 nm diameter and 4–5 nm thickness have been measured by electron microscopy (15). Because of the negative anisotropy of the diamagnetic susceptibility of dialkanoylphospholipids in the whole edifice, $\Delta\chi$ ($\Delta\chi = \chi_{//} - \chi_{\perp}$, where $\chi_{//}$ and $\chi_{\perp}$ respectively represent the magnetic susceptibility parallel and perpendicular to the long lipid axis), bicelles are aligned by high magnetic fields, the normal, n, to the bilayer disk orienting perpendicular to the field direction B_0. Temperature-hydration-composition diagrams for which bicelles made of DMPC (dimyritoylphosphatidylcholine) and DCPC (dicaproylphosphatidylcholine) orient in magnetic fields are now well characterized (15,19). Their domain of existence is encountered for DMPC molar contents varying from 65% to 87%, temperatures in the range 25–45°C, and from 40% to 95% hydration (w/w). These model membranes display many advantages for biomolecular structural studies, especially if their orientation in the magnetic field can be modulated as a real ''molecular goniometer'' (23–25). Although the direction of alignment can be changed under variable-angle rapid sample spinning (26), a uniform and spontaneous alignment of static samples is

Submitted September 19, 2006, and accepted for publication December 5, 2006.

Address reprint requests to Erick J. Dufourc, UMR 5248 CBMN, CNRS-Université Bordeaux 1-ENITAB, IECB, 2 rue Robert Escarpit, 33607 Pessac, France. Tel./Fax: 33-5-4000-2218; E-mail: e.dufourc@iecb.u-bordeaux.fr.

0006-3495/07/06/3949/11 $2.00

doi: 10.1529/biophysj.106.097758

most desirable. Consequently, investigations are conducted to change the natural alignment of the bicelle's normal from perpendicular to parallel relative to B_0. Two approaches have been used to achieve this goal: the first is to use a paramagnetic lanthanide (27–30) such as Eu^{3+}, Tm^{3+}, or Yb^{3+}, but the line broadening promoted by these cations may be a concern. The second is the addition of molecules with a large positive $\Delta\chi$, such as peptides (31) or amphiphilic aromatic compounds (32), because phenyl rings have a strong positive $\Delta\chi$ (33,34). However, large amounts of additive are required to obtain the new orientation and may perturb the membrane. To overcome these problems, Cho and co-workers (35,36) developed a modified phosphatidylcholine (PC), the dodecan oyl-2-(4-(4-biphenyl)butanoyl)-*sn*-glycero-3-phosphocholine (DBBPC), in which one of the aliphatic chains contains a biphenyl unit. This phospholipid has a large positive $\Delta\chi$ that naturally induces the new orientation with the bicelle normal aligning parallel to B_0. It was shown that mixtures of DBBPC/DCPC with a ratio close to 6 can form bicellar solutions that are stable from 10°C to 54°C (35).

In our study, we report a new system of bicelles composed with a peculiar phospholipid TBBPC (tetradecanoyl-2-(4-(4-biphenyl)butanoyl)-*sn*-glycero-3-phosphocholine and DCPC. The C_{12} aliphatic chain of DBBPC was replaced by a C_{14} to be closer to the chain length of natural membrane lipids. Preliminary results have already been reported (37). After synthesizing this new lipid TBBPC, we used wide-line ^{31}P, ^{14}N, and ^{2}H solid-state NMR to evaluate lipid polymorphism and dynamics of this binary system on variation of lipid ratio, temperature, and hydration. We also showed that under fixed conditions of temperature, hydration, and composition, discoidal nano-objects can be observed by freeze-fracture electron microscopy and that x-rays (SAXS) can characterize their specific orientation after alignment in the magnetic field. Diagrams and dynamics of water trapped in TBBPC/DCPC bicelles were also compared to similar data already reported from ''classical'' DMPC/DCPC systems (15,19).

MATERIALS AND METHODS

Chemicals

1,2-Dimyristoylphosphatidylcholine (DMPC), 1,2-dicaproylphosphatidylcholine (DCPC), and lyso-myristoylphosphatidylcholine (lyso-MPC) were purchased from Avanti Polar Lipids (Birmingham, AL); the other compounds were purchased from Sigma-Aldrich Chemicals (St. Quentin-Fallavier, France); all these starting materials were used without further purification. Deuterated water (D_2O) was obtained from Eurisotop (Saint Aubin, France).

Synthesis of the TBBPC lipid

1-Tetradecanoyl-2-(4-(4-biphenyl)butanoyl)-*sn*-glycero-3-phosphatidylcholine (TBBPC) was synthesized by following the procedures used for the preparation of the 1-dodecanoyl-2-BBPC as reported by Tan et al. (36) (see Fig. 1 for the TBBPC synthesis scheme). The product was then purified twice on a flash silica gel column, with $CHCl_3$:CH_3OH:H_2O (65:35:4, v/v) as eluent. Fractions containing the lipid were pooled up and the solvent removed by evaporation and freeze-drying. Finally, a white powder of TBBPC was obtained with a 70% yield: ^{1}H NMR (400 MHz, $CDCl_3$), δ (ppm) 7.49 (*d*, 2)H, Ar), 7.44 (d, 2H, Ar), 7.34 (m, 2H, Ar), 7.24 (m, 2H, Ar), 7.17 (d, 2H, Ar), 5.15 (m, 1H, CH), 4.32 (dd, 1H, CH), 4.20 (m, 2H, $POCH_2CH_2N$), 4.06 (dd, 1H, CH), 3.88 (m, 2H, CH_2OCO), 3.66 (m, 2H, CH_2N), 3.23 (s, 9H, $N(CH_3)_3$), 2.6 (*t*, 2H, CH_2), 2.29 (*t*, 2H, CH_2), 2.17 (*t*, 2H, CH_2), 1.88 (*t*, 2H, CH_2), 1.47 (*m*, 2H, CH_2), 1.15 (*s*, 20H, fatty CH_2), 0.8 (*t*, 3H, CH_3); ^{13}C NMR (400 MHz, $CDCl_3$), δ (ppm): 173.83, 173.08, 141.06, 140.68, 139.12, 129.15, 129.1, 128.98, 128.96, 127.32, 127.13, 70.92, 66.55, 63.66, 63.16, 59.46, 54.63, 34.83, 34.33, 33.87, 32.14, 31.17, 29.90, 29.87, 29.75, 29.58, 29.53, 29.37, 26.74, 25.08, 22.91, 14.35; mass spectrum (ESI, full ms): *m*/*z* 689.5 (calculated 689); FT-IR (analysis was performed in between two ZnSe pellets, with TBBPC liposomes hydrated in water, and data were recorded with an OPUS IFS 55 Bruker), $\nu_{stretching}$ (cm^{-1}): 2923 ($CH_{2,\ asym}$), 2852 ($CH_{2,\ sym}$), 1732 (C=O), 1378 (O=C–CH_3), 1229 (O–C=O), 1087 and 1067 (O–CH_2).

Bicelles preparation

For ^{31}P or ^{2}H NMR experiments, appropriate amounts of phospholipids were weighted to obtain mole contents, *X*, of TBBPC in the mixture ranging from 80% to 95% (molar ratio q = [TBBPC]/[DCPC] varying from 4 to 19). A suitable volume of deuterated water, D_2O, containing 100 mM NaCl was added to obtain a lipid hydration, *h*, ranging from 70% to 95% (w/w). Hydration is defined as the mass of water over the total mass of the system (phospholipids and water). Hydrated samples were centrifuged at 6500 rpm for 5 min and vigorously stirred in a vortex mixer. The samples were then frozen in liquid nitrogen for 30 s, heated at 50°C for 10 min in a water bath, vigorously stirred in a vortex, and centrifuged again at 6500 rpm for 5 min. This cycle was repeated three times until a viscous (milky or translucent, depending on *X*) suspension was obtained at room temperature. Each preparation was then transferred into a 4-mm NMR tube (80 μl, ZrO_2 rotor) for wide-line NMR experiments; the less hydrated samples (h = 70%) were transferred in the rotor according to the following procedure: hydrated samples were prepared in a conical plastic microtube (1.5 ml) that was frozen in liquid nitrogen and then transferred into the 4-mm rotor using a home-made funnel. The latter allows filling the rotor homogeneously, without air bubbles, with centrifugation at 2000 rpm for 30 s at room temperature. For ^{14}N NMR experiments, DMPC/DCPC and TBBPC/DCPC systems were prepared with X = 78% in 100 mM KCl and X = 85.7% in 100 mM NaCl, respectively, with a total lipid hydration of 90% (w/w) in D_2O. The same sample preparation, as described above, was applied. For electron microscopy analyses, TBBPC/DCPC mixtures were prepared with h = 90% and X = 85.7%. For SAXS analyses, TBBPC/DCPC bicelles were prepared with h = 80% and X = 87.5%.

NMR spectroscopy

NMR experiments were carried out on Bruker Avance 500-, 400-, and 300-MHz spectrometers. ^{31}P NMR spectra were acquired at 162 MHz, using a phase-cycled Hahn-echo pulse sequence with gated broadband proton decoupling (38). ^{2}H NMR experiments on deuterated water were performed at 61.5 MHz and 46 MHz, by means of a one-pulse sequence. ^{14}N NMR experiments were acquired at 36 MHz, using a quadrupolar echo pulse sequence (39). Typical acquisition parameters were as follows: spectral window of 32 kHz for ^{31}P NMR, 2 kHz for ^{2}H NMR, and 100 kHz for ^{14}N NMR; $\pi/2$ pulse widths of 14.5 μs for ^{31}P NMR, 17 μs for ^{2}H NMR, and 10 μs for ^{14}N NMR; interpulse delays were of 50 μs for ^{31}P NMR and 200 μs for ^{14}N NMR. A recycle delay of 5 s was used for ^{31}P and ^{2}H NMR, and for ^{14}N NMR experiments it was set to 0.2 s. Typically, 350 scans were recorded for phosphorus spectra with deuterium (D_2O) lock, 40 scans for deuterium spectra, and 40,000 scans for nitrogen spectra. A line broadening of 50 Hz was usually applied before Fourier transformation for phosphorus spectra, from 2 to 5 Hz for ^{2}H NMR experiments, and from 20 to 100 Hz for ^{14}N RMN. Quadrature detection was used in all cases. Samples were allowed to equilibrate at least 30 min at a given temperature (ranging 0°C to 80°C for TBBPC bicelles) before the NMR signal was acquired; the temperature was regulated to $\pm$1°C. All the

thermal variations were performed by increasing the temperature from 25°C to 80°C and by decreasing the temperature from 25°C to 0°C.

Freeze-fracture electron microscopy

Freeze-fracture experiments were performed with a Balzers BAF 300 vacuum chamber (Balzers, Liechtenstein). A small droplet of the TBBPC/DCPC preparation was sandwiched between two copper specimen holders at room temperature. The sandwich was then frozen with liquid propane cooled with liquid nitrogen. The frozen sandwich was additionally fixed to a transport unit under liquid nitrogen and transferred to the fracture replication stage in a chamber that was then pumped down to 2×10^{-6} mBar at -145°C. Immediately after fracturing, replication took place by first shadowing with platinum/carbon at a 45° angle and then with carbon deposition at 90°. The sample was then allowed to warm at room temperature. Replicas were retrieved from the fractural plane and cleaned in ethanol/water (2:1, v/v) and mounted on 300-mesh copper grids. Observations were made with a transmission electron microscope FEI EM120 operated at 120 kV. Images were recorded using a SSCCD 2k × 2k Gatan camera. The Corel Photo Paint package was used for image processing. The Scion software was used to measure bicelle size on TEM images, considering each time the longest dimension of the objects. A histogram was built from these measurements and analyzed by a Gaussian function with Origin software.

Small-angle x-ray scattering

A Rigaku Nanoviewer (Micro-source generator, MicroMax 007, Tokyo, Japan) was used, equipped with a rotating Cu anode generator operated at 40 kV and 20 mA, coupled with a Confocal Maxflux Mirror. The two-dimensional scattering pattern was measured using a Mercury CCD camera, and the distance sample-detector was fixed to 425 mm ($0 \leq q \leq 0.35$ Å^{-1}). The solutions were sealed in glass capillaries with a 1.5 mm diameter (Glaskapillaren GLAS, Germany) and placed in the sample chamber regulated at 35°C. The exposure time was 600 s, and the scattering intensities from the buffer solution as well as the detector dark were measured separately and subtracted from that of samples. The obtained two-dimensional scattering patterns were analyzed with Rigaku Nanoviewer software, which allows an integration of the signal intensity either circularly (over 360°) or linearly (at 0° or 90°). The resulting data were then treated with Origin software.

RESULTS

In the first section, the binary system TBBPC/DCPC is described: after the TBBPC synthesis several samples of the mixture were prepared by varying the mole fraction of TBBPC, X, the temperature, T, and the hydration, h, and diagrams were further established using phosphorus wide-line NMR. The TBBPC/DCPC disk size was statistically determined on TEM images and compared with that obtained from integration of NMR lines (15,31). Their specific orientation with the bilayer normal, n, parallel to the magnetic field, $n//B_0$, was confirmed by SAXS analysis after alignment in B_0. In a second part, the biphenyl bicelles are compared with their chain saturated analogs (DMPC/DCPC system): ^{14}N NMR, ^{2}H NMR (of deuterated water), and temperature-composition domains.

Biphenyl bicelles

TBBPC synthesis

The TBBPC phospholipid was successfully synthesized (Fig. 1) with a satisfactory yield (70%). The esterification

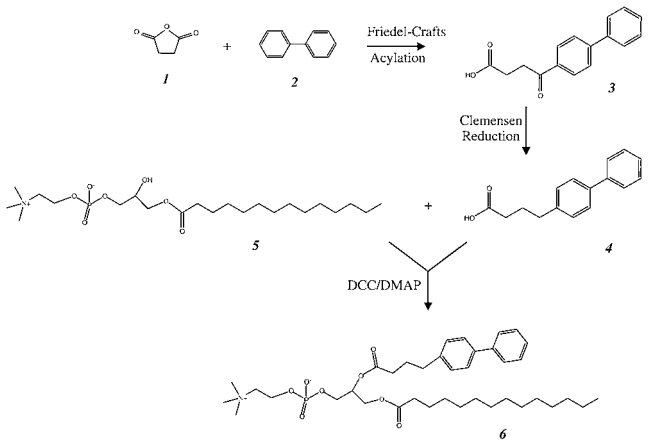

FIGURE 1 Synthetic reaction scheme for the TBBPC phospholipid, obtained from an esterification reaction between 1-myristoyl-2-hydroxy-*sn*-glycero-3-phosphocholine and the 4-(4-biphenyl)butanoic acid; this last one was previously synthesized by a Friedel and Craft acylation and a Clemmensen reduction (36). 1, succinic anhydride; 2, biphenyl; 3, 4-(4-biphenyl)-4-oxobutanoic acid; 4, 4-(4-biphenyl)butanoic acid; 5, 1-myristoyl-2-hydroxy-*sn*-glycero-3-phosphocholine; 6, 1-tetradecanoyl-2-(4-(4-biphenyl)butanoyl)-*sn*-glycero-3-phosphatidylcholine (TBBPC).

reaction between the lyso-lauroylphosphatidylcholine (C_{12} aliphatic chain) and the 4-(4-biphenyl)butanoic acid (60% yield) (36), can easily be applied and with a better yield to a myristoylphosphatidylcholine (C_{14} aliphatic chain), whose chain length is closer to that of natural membrane lipids.

^{31}P NMR spectroscopy of TBBPC-DCPC binary systems (depending on X and h)

Samples with TBBPC mole fractions ranging from $X = 80\%$ to $X = 95\%$ were prepared with two different hydration conditions, $h = 80\%$ and $h = 90\%$, in the presence of 100 mM NaCl. For most combinations of individual lipid composition and hydration, the temperature was varied from 0°C to 80°C. Figs. 2 and 3 show selected spectra for the different TBBPC/DCPC binary systems relative to mole fraction of TBBPC, X (for $h = 80\%$, Fig. 2), temperature and hydration (for $X = 86\%$, Fig. 3). These spectra display a wide variety of line shapes that are characteristic of pure lipid phases or of a mixture of lipid phases. It must be mentioned here that the term ''phase'' is used in this report to qualify a change in polymorphism as detected by NMR, which may not necessarily correspond stricto sensu to the Gibbs thermodynamic definition. Fig. 2 spectra corresponding to $X = 80\%$ and $T \geq 40$°C exhibit a single sharp line centered at 0.9 ppm, close to the isotropic chemical shift of phosphatidylcholine. This single line reflects the total averaging of the chemical shift anisotropy interaction because of the presence of small and rapidly tumbling objects (mixed micelles or very small bicelles). Several spectra present two sharp lines with a chemical shift of ~20 ppm and ~5 ppm (see for instance Fig. 2: $X = 85.7\%$ for $T = 50$°C and $X = 87.5\%$ from $T = 25$°C to $T = 70$°C; or Fig. 3: $X = 86\%$, temperatures varying from 10°C to 50°C and hydration varying

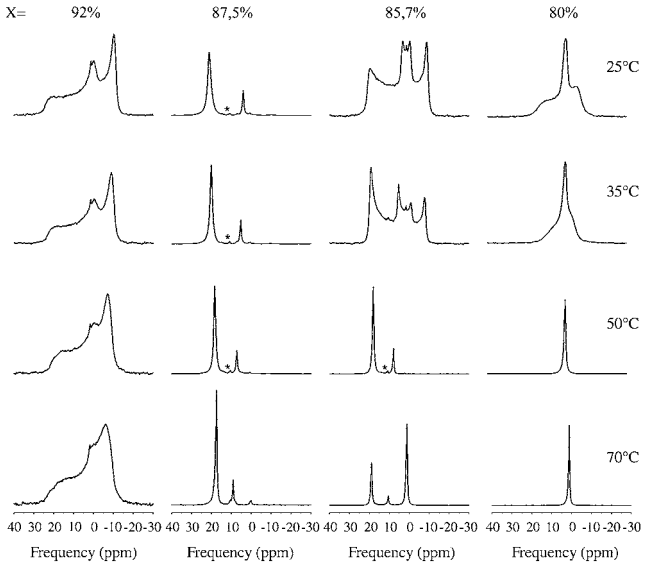

FIGURE 2 Gated proton-broad band decoupled ^{31}P NMR spectra of TBBPC/DCPC binary mixtures in 80% D_2O (w/w), 100 mM NaCl. Mole fractions X = [TBBPC]/([TBBPC] + [DCPC]) are indicated on the top. Temperature is indicated on the right hand side of spectra. Each spectrum is the average of 350 scans.

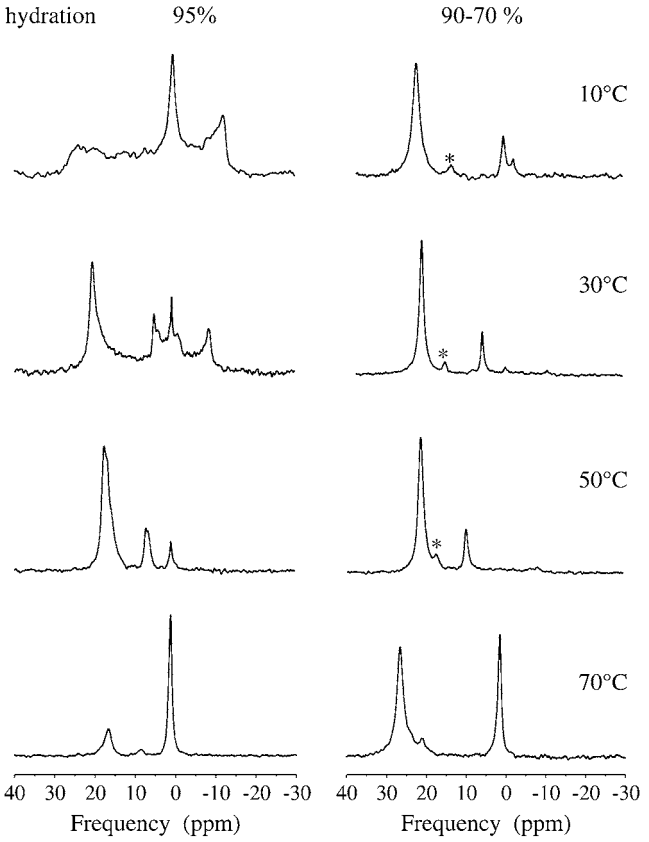

FIGURE 3 Gated proton broad band decoupled ^{31}P-NMR spectra of TBBPC/DCPC binary mixtures in D_2O, 100 mM NaCl for X = 86%. Hydration content is indicated on the top. Hydration, h, is defined as the mass of water over the total mass of the system (phospholipids and water). Temperature is indicated on the right-hand side of spectra. Each spectrum is the average of 350 scans.

between 70% and 90%). These particular spectra are the signature of bicelles oriented with their normal to the bilayer parallel to the magnetic field: the major peak may be assigned to phospholipids located in the bilayer plane with their director axis oriented parallel to B_0 (assigned to TBBPC in the majority), whereas the smaller peak results from the rapid diffusion of lipids on the highly curved surface at the edge of the bicellar disk (assigned mainly to DCPC). Moreover, we can notice in Fig. 2 that for $X = 87.5\%$ and temperatures varying from 10°C to 70°C, the more the temperature increases, the more the distance between the two lines decreases, and the sharper the peaks become, which may be associated with a better macroscopic orientation of the system in the field (15). For $X = 85.7\%$, $T = 70$°C, $h = 80\%$ (Fig. 2) and for $X = 86\%$, $T = 50$–70°C, $h = 95\%$ (Fig. 3), these bicelles coexist with an isotropic phase. For $X \geq 92\%$ with the temperature varying from 25°C to 70°C and $X = 80\%$ for $T = 25$°C and 35°C (Fig. 2), we mainly observe composite spectra with a superimposition of an isotropic line and a broad axially symmetric powder pattern (for $T = 25$°C, $\Delta\sigma = 17.5$ ppm for $X = 80\%$ and $\Delta\sigma = 33$ ppm for $X = 92\%$). The broad spectrum is characteristic of an unoriented lamellar phase. Most of the other spectra combine the superposition of two or three of the spectral features that correspond to micelles, oriented bicelles, or lamellar phases. For example, for $h = 70$–90% and $T = 70$°C (Fig. 3, $X = 86\%$), an isotropic phase coexists with an oriented lamellar phase (whose normal is oriented in majority parallel to B_0). We can also point out the case for $X = 85.7\%$ and a temperature below 35°C (Fig. 2), where the spectrum shape is quite odd. We performed spectral simulations (not shown) and could well account for the shape assuming a cylindrical symmetry (tubes) (40,41) or using a vesicle of prolate form oriented perpendicular to the field (42). Because we could not go further in assignment, and because more detailed studies (outside the scope of our study) clearly would have been needed to explore this domain of temperature and composition, we cannot comment further on such shapes.

Temperature-composition diagrams of TBBPC/DCPC binary systems

Following Raffard and Aussenac and their associates (19,43), analysis of ^{31}P NMR spectra may be used to build temperature-composition diagrams of TBBPC/DCPC for the two different hydration conditions, $h = 80\%$ and $h = 90\%$, studied in the presence of 100 mM NaCl (Fig. 4). Domains where a single spectral feature is detected are indicated in Fig. 4 by bold letters as **I** (isotropic phase, mixed micelles, or very small bicelles), **B** (magnetically oriented bicelles), and **L** (lamellar phase). A solid line as eye guide delimits the domain where bicelles orient in the magnetic field. The TBBPC/DCPC bicelles exist on a wide temperature span (from 10°C to 70°C for $h = 80\%$ and from 10°C to 60°C for $h = 90\%$) but for a narrow range of lipid composition (from 85.7% to 88.9% for $h = 80\%$ and from 84%

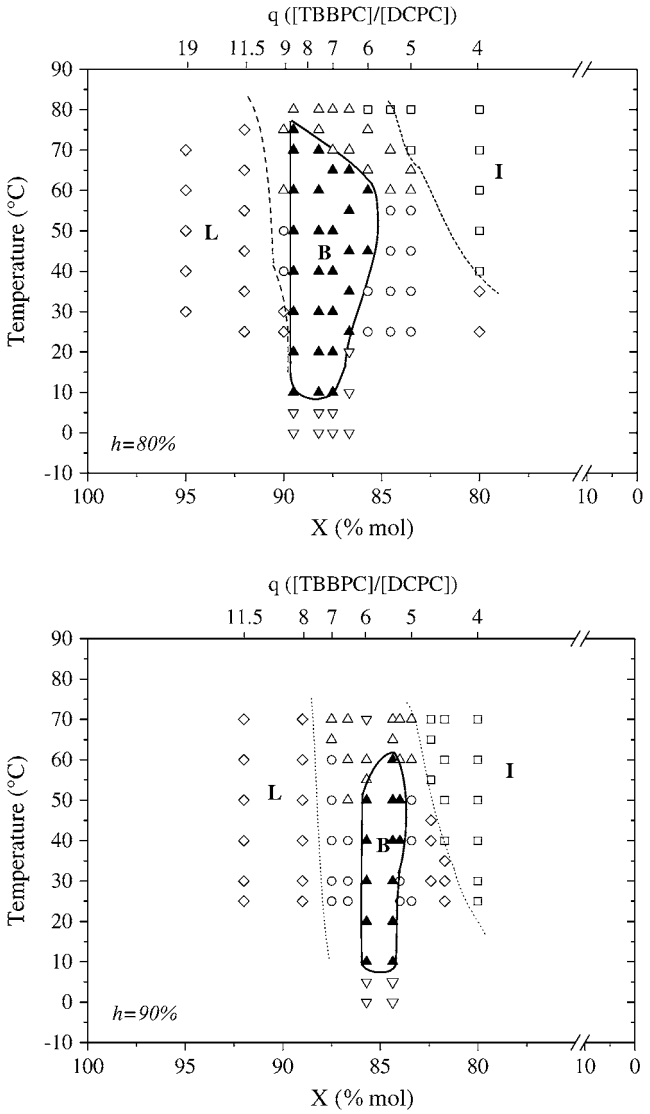

FIGURE 4 Temperature-composition diagrams of TBBPC-DCPC system for two selected hydration contents ($h = 80\%$, *top*, and $h = 90\%$, *bottom*), in the presence of 100 mM NaCl as determined from ^{31}P NMR spectra: (▲) single phase of bicelles oriented by the magnetic field; (Δ) oriented bicelles coexisting with isotropic or unoriented phase; (○) composite phase with cylindrical symmetry; (∇) isotropic phase coexisting with an oriented lamellar phase; (□) isotropic phase; (◇) lamellar phase. Mole fractions X are expressed in percentage; the corresponding ratio q = [TBBPC]/[DCPC] is indicated with a double x-scale on top. Single-phase regions are denoted I, B, and L for isotropic, magnetically oriented bicelles, and lamellar phases. Solid and dashed lines respectively delineate purely magnetically oriented bicelle domains from purely lamellar or isotropic phases.

to 86% for $h = 90\%$). Therefore, with increasing hydration, the oriented bicelle domain is reduced a little and shifted toward smaller X values. For each hydration condition investigated, bicelles are surrounded by an isotropic domain for low X values and by a lamellar phase for high TBBPC compositions. Two–phase regions, as a function of temperature, are observed above and below the bicellar domain. They are composed of an isotropic phase coexisting with an oriented lamellar phase for low temperatures and bicelles or an oriented lamellar phase coexisting with an isotropic phase for high temperatures. Adjacent to the bicelles' existence domain, a phase mixture with spectra (Fig. 2, *top*, 85.7%) that may represent objects with cylindrical or oblate vesicle symmetry is observed (vide supra).

Freeze-fracture electron microscopy and bicelle size

Samples of TBBPC/DCPC bicelles with $X = 85.7\%$ and $h = 90\%$ (with 100 mM NaCl) were observed by freeze-fracture transmission electron microscopy. A representative TEM image is shown in Fig. 5 *A*, where a reasonable monodisperse ensemble of discoidal nano-objects is observed. These appear with either a white or gray coloration, depending on their initial orientation in the sample before the fracture (the shadowing being at 45°): explicative schemes (Fig. 5 *B*) show that an object parallel to the fracture surface will appear in average gray, whereas a perpendicular one will appear white. The uniform color of the object confirms their discoidal form with a flat area (a spherical object would appear with a pronounced

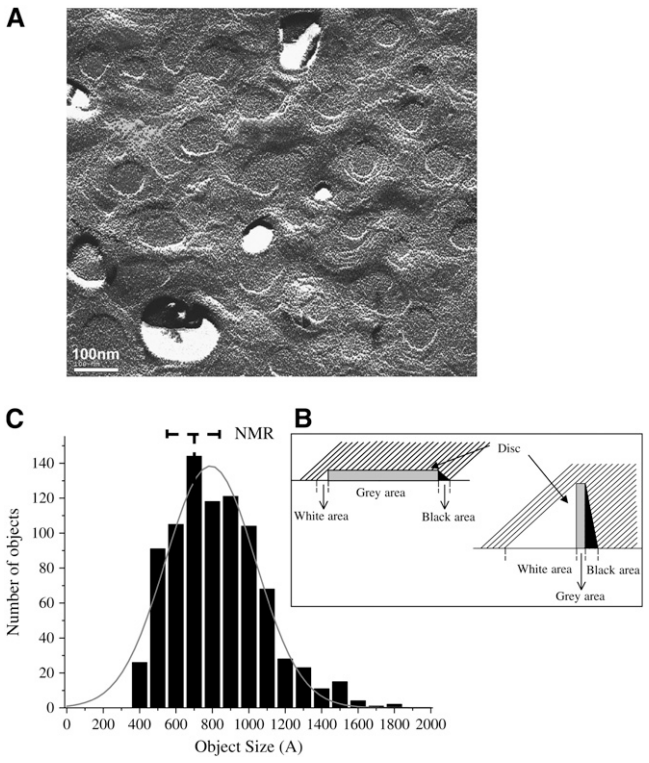

FIGURE 5 (*A*) Freeze-fracture electron microscopy image of the TBBPC/DCPC system ($X = 85.7\%$, $h = 90\%$ in D_2O (w/w) containing 100 mM NaCl). The sample was frozen from room temperature. The bar in the picture measures 100 nm. (*B*) Schematic drawing showing the resulting shadows (45°) when a bilayered disk is either parallel or perpendicular to the fracture plane. (*C*) Histogram of size distribution for the TBBPC/DCPC system ($X = 85.7\%$, $h = 90\%$ in D_2O with 100 mM NaCl). Objects were measured on the electron microscopy images, considering each time their longest dimension. Histogram was built with a frequency count for object size of 100 Å and analyzed by a Gaussian function (*solid line*). A comparison with the size determined from ^{31}P NMR data is indicated (*dashed line*).

gradation from black to white). The longest dimension of 860 anisotropic objects, coming from two replications, was measured on the collected TEM images, and a size histogram was built using a step size of 100 Å (Fig. 5 *C*) and fitted with a Gaussian function (*solid bold line*) to characterize the mean size. An average diameter of 790 Å, with a half-width at half-height of 300 Å was obtained. The statistical size of TBBPC/DCPC bicelles, measured on TEM images, can be compared to that obtained from ^{31}P NMR data by directly integrating the area under the two sharp peaks, assigned to lipids in the flat area and in the half-torus of the disk (15,31). Although this method is rough and also caused by the presence of very small peaks on NMR spectra (tentatively attributed to impurities from possible chain scrambling during synthesis (44), and noted as *asterisks* on spectra), which made it difficult to accurately perform peak integration, an approximate size of 700 ± 100 Å was found from the ^{31}P NMR data ($T = 25$°C), which are in very good agreement with the statistical size determined on TEM images.

Small-angle x-ray scattering of magnetically oriented bicelles

A 1.5-mm-diameter glass capillary was filled with 30 μl of a TBBPC/DCPC bicelles preparation ($X = 87.5\%$, $h = 80\%$ in 100 mM NaCl) and sealed. This capillary was placed in a rotor, and the whole was set in the NMR probe, regulated at 35°C, so that the capillary is aligned with the magnetic field direction. After 20 min in the magnetic field (11.74 Tesla), the capillary was transferred in a 35°C water bath, in ~2 min, and then mounted in the SAXS apparatus, previously regulated at 35°C. X-ray data were acquired in 10 min and are shown in Fig. 6 *A* (*right*). As can be seen, the resulting 2D scattering pattern consists of four spots aligned along the *z*-direction, which characterizes a bilayer normal orientation parallel to B_0 ($n//B_0$). A control experiment was performed with the same sample without magnetic orientation and shows a classical circular pattern, typical of nonoriented material (Fig. 6 *A*, *left*). These two-dimensional scattering patterns are integrated to yield the $I = f(q)$ graph (where I is the scattering intensity and q the scattering vector in reciprocal angstroms). Integration is performed as described in Materials and Methods, i.e., over 0–360° for nonoriented systems and along the direction parallel (*z* axis) to the magnetic field (see Fig. 6 *A*) for systems having been oriented in the field. Hence, $I = f(q)$ patterns for nonoriented bicelles (*dashed line*, intensity × 40) and magnetically oriented bicelles (*solid line*) are shown in Fig. 6 *B*. A wide peak is found for both nonoriented and oriented bicelles, which is characteristic of a phospholipid bilayer structure (45–48). For oriented bicelles, a Bragg peak is found for $q = 0.055$ Å^{-1}, which corresponds to a periodicity of 114 Å. This Bragg peak is not detected for nonoriented bicelles, as they are dispersed in all directions. It is also noticeable that the intensity of the magnetically oriented TBBPC/DCPC bicelles is much higher (factor 40) than that of the nonoriented ones: in the first case, all the objects are orienting in the same direction and participate in the x-ray scattering, whereas, in the second case, the bicelles have no specific orientation, therefore decreasing the number of bicelles participating in the coherent x-ray scattering.

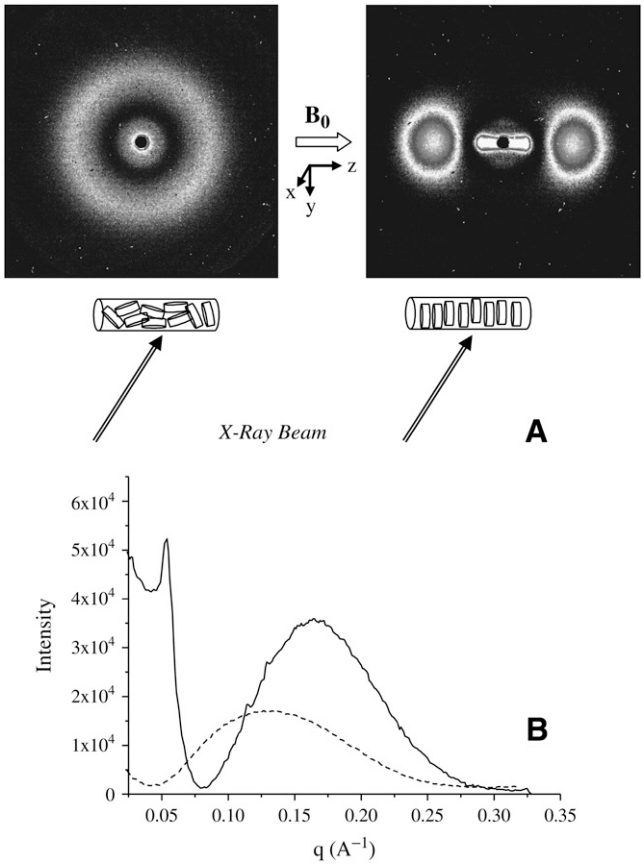

FIGURE 6 (*A*) SAXS images of TBBPC/DCPC bicelles ($X = 87.5\%$) before (*top left*) and after (*top right*) orientation for 20 min in an 11.7-Tesla magnetic field (B_0) at 35°C. The drawings below are to help elucidate the position of the capillary tube in the x-ray setup. (*B*) $I = f(q)$ profile of TBBPC/DCPC bicelles without orientation in B_0 after a circular integration in the (*yz*) plane (*dashed line, scale ×40*), and TBBPC/DCPC bicelles after orientation in B_0 (*solid line*, linear integration relative to the *z* axis).

TBBPC/DCPC versus DMPC/DCPC bicelles

^{14}N NMR spectroscopy of TBBPC/DCPC and DMPC/DCPC binary systems

^{14}N NMR can also be applied on bicelle systems because they provide information about the dynamics of the choline head group. DMPC/DCPC and TBBPC/DCPC mixtures were prepared with 90% hydration ($X = 80\%$ and $X = 85\%$, respectively), and the temperature was varied from 0°C to 70°C. Selected spectra for the two systems are shown in Fig. 7. The DMPC/DCPC binary system exhibits three different spectral features, as a function of temperature: below 20°C, a sharp peak, centered at 0 Hz is observed and reflects an isotropic phase. Between 30°C and 40°C, DMPC/DCPC present two distinct quadrupolar splittings, $\Delta\nu_Q$, which characterize bicelles oriented with their normal perpendicular to the field; the smaller (1.68 kHz at 30°C) is assigned to lipids in the

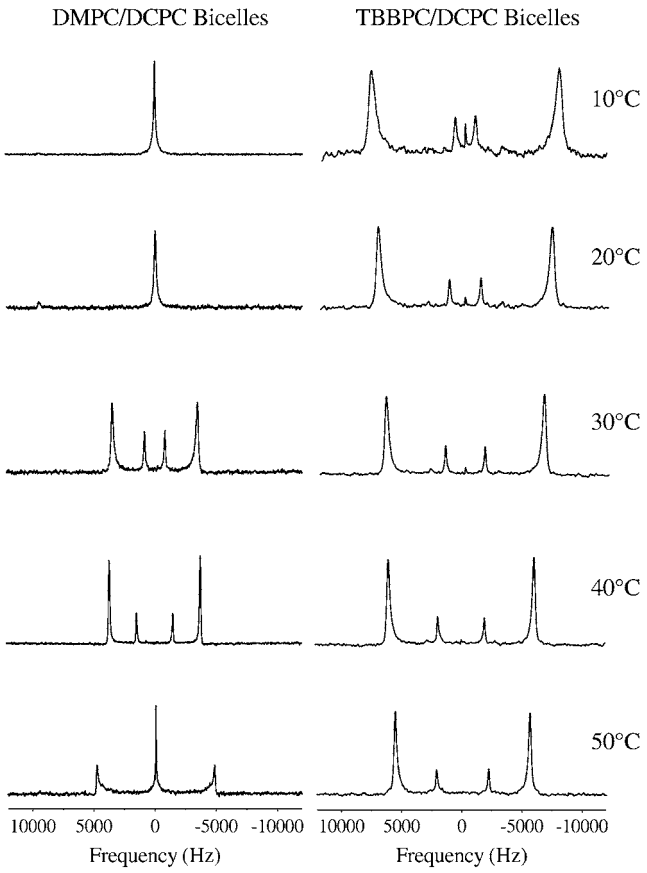

FIGURE 7 ^{14}N NMR spectra of DMPC/DCPC bicelles and TBBPC/DCPC bicelles in 80% D_2O (w/w) containing, respectively, 100 mM NaCl and 100 mM KCl, $X = 78\%$ for DMPC/DCPC, and $X = 87.5\%$ for TBBPC/DCPC. Temperature is indicated on the right hand side of spectra. Each spectrum is the average of 40,000 scans.

disk edge (half-torus part, mainly DCPC), and the larger (6.96 kHz at 30°C) to lipids in the flat bilayer (mainly DMPC). Above 40°C, an isotropic line is observed coexisting with a large quadrupolar splitting (9.62 kHz), specific for a lamellar phase showing residual magnetic field orientation. The TBBPC/DCPC binary system exhibits the characteristic spectral feature of oriented bicelles for all the temperatures studied, which is in agreement with the bicelle domain determined by ^{31}P NMR. The smallest quadrupolar splitting (3.27 kHz at 30°C) is assigned to lipids in the toroidal part (mainly DCPC), and the largest (13.17 kHz at 30°C) to lipids in the disk (mainly TBBPC). We can notice that on increasing temperature, the outer splitting becomes narrower, whereas the inner increases. It is interesting to remark that quadrupolar splittings corresponding to the TBBPC/DCPC system are nearly twice as large as those of DMPC/DCPC, at the same temperature. This is clearly related to the $(3\cos^2\beta - 1)/2$ relation that is bound to the quadrupolar splitting equation (41,49), where β is the angle between the bilayer normal and the magnetic field direction: for ''classical'' bicelle systems $\beta = 90°$, whereas $\beta = 0°$ for the biphenyl analog. Finding a ratio of ~2 between TBBPC/DCPC and DMPC/DCPC quadrupolar splittings is also an indirect control of a change in magnetic orientation by 90° on going from one system to the other. A more detailed look at this ratio indicates that it is slightly lower than 2, suggesting that the choline head group in TBBPC possesses a slightly greater motional freedom or a slightly different orientation in comparison to that in DMPC.

^{2}H NMR spectroscopy of D_2O in TBBPC/DCPC binary systems

Water structure and dynamics were investigated by replacing H_2O by deuterated water, D_2O, in some samples studied by phosphorus NMR. ^{2}H NMR spectra were recorded for three hydration contents (70%, 80%, and 90%) over a large temperature variation (from 0°C to 80°C) with $X = 86\%$. For all hydration contents, a single small quadrupolar splitting is detected for temperatures ranging from 10°C to 70°C. This reflects water molecules that are oriented on average around the bicelles, in concordance with the oriented bicellar domains established by ^{31}P NMR for $h = 80\%$ and $h = 90\%$ (see Fig. 4). Fig. 8 reports the D_2O quadrupolar splitting in the biphenyl bicelles as a function of temperature and hydration. The quadrupolar splitting values range from 13 Hz to 186 Hz: for a fixed TBBPC mole fraction, it increases with temperature and with dehydration. A comparison with the D_2O quadrupolar splittings observed in DMPC/DCPC bicelles, reported by Arnold et al. (15), is plotted for $h = 80\%$ ($X = 78\%$), in Fig. 8. For chain-saturated bicelles, $\Delta\nu_Q$ varies from 24 Hz at 30°C to 46 Hz at 39°C, whereas for biphenyl bicelles, it varies from 74 Hz at 30°C to 85 Hz at 40°C. The values for the biphenyl system are more than twice as large, which is again related to the specific orientation of each type of bicelle (it induces at least a

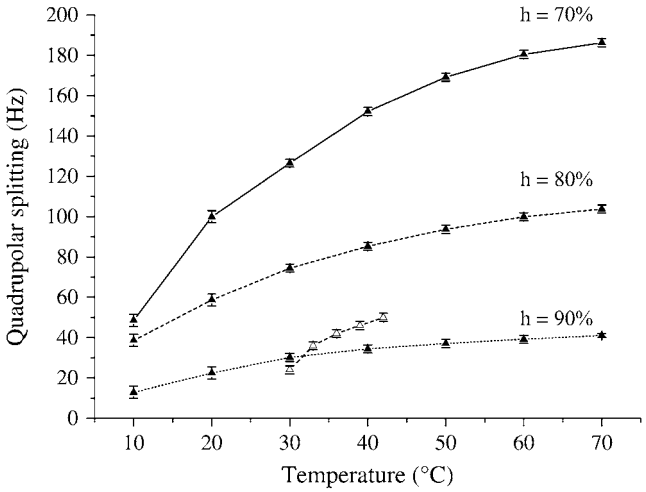

FIGURE 8 Quadrupolar splitting (Hz) of deuterated water in TBBPC/DCPC mixtures (containing 100 mM NaCl for $X = 86\%$) as a function of the temperature (°C) for 70% (*solid line*), 80% (*dashed line*), and 90% (*dotted line*) hydration. These results are compared to those of DMPC/DCPC bicelles for $h = 80\%$ (Δ), reported by Arnold et al. (15).

factor 2 between the quadrupolar splittings). This is particularly interesting for structural studies where soluble molecules are trapped in the organized water medium: one will thus measure more accurately residual dipolar couplings on a wider thermal span (10–70°C).

TBBPC/DCPC versus DMPC/DCPC diagrams

The composition-temperature and temperature-hydration diagrams established for TBBPC/DCPC system can be directly compared to those of DMPC/DCPC system, reported by Raffard et al. (19). Fig. 9 *A* reports the superposition of the temperature-composition domains for which magnetic field orientation occurs, at a fixed hydration, $h = 80\%$. The labels $B_{//}$ and $B_{\perp}$ respectively stand for bicelles with a normal oriented parallel or perpendicular to the field. Interestingly, the two systems reflect marked differences: whereas DMPC/DCPC oriented disks are found for DMPC contents varying from 87% to 65%, TBBPC/DCPC oriented disks are encountered for only a narrow range of compositions, namely $X = 85.7\%$ to $X = 88.9\%$. However, the range of temperatures where they are aligned with their normal parallel to the field spans from 10°C to 75°C, whereas for DMPC/DCPC this happens only between 25°C and 45°C. Fig. 9 *B* reports the superposition of the temperature-hydration domains at a fixed long-chain lipid content, $X = 86\%$. The same symbols as in Fig. 9 *A* are used. It points out the high stability in temperature of TBBPC/DCPC oriented systems compared to DMPC/DCPC ones. The first ones exist from 10°C to 70°C for 70% hydration, whereas the second ones exist from 30°C to 44°C. In both cases, the more hydrated the sample, the more reduced the bicelle domain. Nevertheless, DMPC/DCPC magnetic field orientation is found only from 35°C to 42°C at 90% hydration, whereas TBBPC/DCPC bicelles are still orientable from 10°C to 55°C. For hydration >95%, the two types of bicelles no longer orient in B_0.

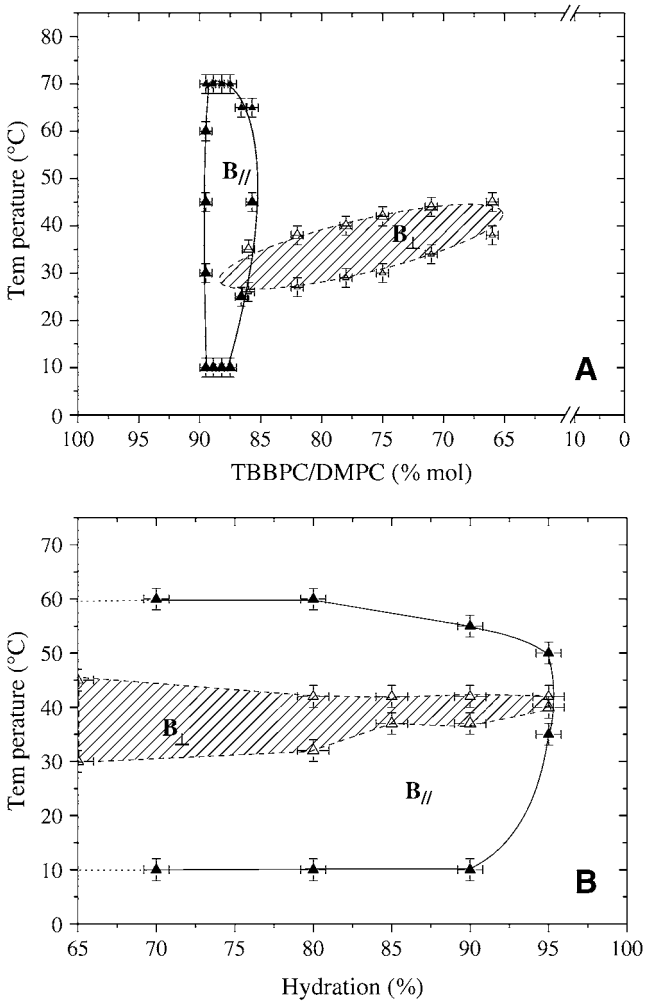

FIGURE 9 (*A*) Temperature-composition diagrams of DMPC/DCPC (*dashed line, hatched area*) and TBBPC/DCPC (*solid line*) in 80% (w/w) D_2O, 100 mM KCl and 100 mM NaCl, respectively, and (*B*) temperature-hydration diagrams for DMPC/DCPC ($X = 78\%$, 100 mM KCl) TBBPC/DCPC bicelles ($X = 85.7\%$, 100 mM NaCl) as determined by phosphorus NMR. Only magnetic field-oriented bicellar domains are indicated: (Δ) DMPC system, (▲) TBBPC system. Lines are drawn as eye guides to delineate domains. $B_{//}$ and $B_{\perp}$ respectively stand for disk normal oriented parallel or perpendicular to the field. DMPC/DCPC data are taken from Raffard et al. (19).

It is also noticeable that biphenyl bicelles show a better stability in time than saturated chains' bicelles: indeed, they show their characteristic oriented spectrum even after 1 mo (or more, if they are conserved in the refrigerator at 4°C, spectra not shown), whereas DMPC/DCPC bicelles lose their oriented spectra after 2 wk. This is mainly because of the slow hydrolysis of lipids, a phenomenon that can be reduced if the ester function is replaced by an ether (43).

DISCUSSION

In this study, two groups of results appear, the first concerning the physical properties of TBBPC/DCPC systems characterized by wide-line NMR spectroscopy, freeze-fracture electron microscopy, and SAXS, and the second comparing these new bicelles with the well-characterized DMPC/DCPC bicelles. They are discussed sequentially in the following.

Biphenyl rings lead to $n//B_0$ oriented bilayered disks with high temperature stability

Major results have been found: 1), disks ~800 Å have clearly been evidenced by freeze-fracture electron microscopy, 2), they can be oriented by magnetic fields in a smectic-like arrangement, i.e., with their normal parallel to the field, and 3), the macroscopic orientation is sufficiently stable that it can be transported and studied by x-rays where the oriented pattern is clearly demonstrated. The morphology of bicellar mixtures is very diverse and has been subject to debate in the last decade. Disk-shaped, cylindrical ''wormlike'' micelles and perforated lamellae have been reported (15–22). Because systems have been mostly studied by solid-state NMR and

small-angle neutron scattering (SANS), with which it may be subtle to distinguish between oriented disks and oriented perforated lamellae, the controversy went until TEM disk images could be taken for the DMPC/DCPC system with different cations (15). In fact, the morphology of mixtures of long-chain and short-chain lipids is so rich that disks and cylindrical ''wormlike'' micelles can be found with the same system but for different conditions of composition, temperature, or hydration. In our work, the observation of TBBPC/DCPC disks by freeze-fracture electron microscopy rules out the presence of perforated lamellae: in the latter case, the holes on TEM images will appear with a gray coloration as for the membranes, and the coexistence of gray and white pictures, as observed in our case, would not be possible. From these TEM images, an average size of 790 Å has been statistically determined, which is nearly twice that found for the DMPC/DCPC system (~450 Å). This clearly scales with the lipid molar ratio q (=[long-chain lipid]/[short-chain lipid]) that is 3.5 for DMPC/DCPC and 6 for TBBPC/DCPC: the greater the q, the larger the disk diameter. A rough geometric model has been in fact proposed in which the disk diameter, Φ, can be deducted from q, assuming that long-chain and short-chain lipids segregate in the disk plane and in the half-torus, respectively ($\Phi = aq(\pi + (\pi^2 + 8/q)^{1/2}) + 2a$) (15,31). By taking $2a \approx 40$ Å, the bilayer thickness of C_{14} phospholipids (50–52), one would calculate a theoretical diameter of ~820 Å for biphenyl bicelles ($q = 6$). These values are somewhat larger than the diameter of the disks, 700 Å, found from integration of NMR lines. However, taking into consideration that the two lipids probably do not completely segregate in plane and torus areas, we can still conclude that the two techniques agree well on determining the bicelle sizes. Consequently, there is a direct link between the lipid composition and the bicelle size.

Of great interest is the fact that bicellar disks, once oriented 20 min in the sufficiently strong magnetic field, keep their macroscopic orientation for several days and can be studied by SAXS outside the magnetic field. This technique nicely confirms the specific orientation of TBBPC/DCPC bicelles such that their normal is parallel with the field, $n//B_0$, the resulting two-dimensional scattering pattern exhibiting well-defined spots in the $z//B_0$ direction. Consequently, SAXS can be used as a good alternative to NMR to specify the orientation of systems such as bicelles. The minimum magnetic field needed for such macroscopic orientation has not been determined yet. For DMPC/DCPC systems doped with lanthanides, 1 Tesla appeared to be enough for these bicelles (53). Experiments with smaller magnetic fields would be interesting to see whether the TBBPC biphenyl rings help in the orienting capabilities of bicelles, i.e., weaker fields might be sufficient. The broad peak obtained for the $I = f(q)$ profile characterizes the phospholipid bilayer structure of the objects, as suggested by Riske et al. (48). A repeat distance of 114 Å between two oriented TBBPC/DCPC disks has been determined by analyzing the Bragg peak on the $I = f(q)$ curve (Fig. 6 *B*). Interestingly Katsaras et al. clearly evidenced a smectic arrangement for DMPC/DCPC systems doped with Tm^{3+} with a comparable lamellar spacing (116 Å for 77% hydration) (53). Given the DMPC maximum hydration with a ~60 Å repeat distance, in the absence of charged additives, such periodicities confirm the high hydration of the sample, which makes this system an attractive model membrane for structural studies where proteins are embedded in the water medium.

For the first time, solid-state NMR was performed on TBBPC/DCPC mixtures. It must be mentioned here that Cho and co-workers also reported ^{31}P NMR data on somewhat shorter (C_{12}) biphenyl bicelles (DBBPC/DCPC) (35,36). We basically find the same NMR features as they reported: ^{31}P NMR spectra made of two sharp peaks with positive chemical shifts, indicative of bilayer normal oriented parallel to the magnetic field direction, the highest peak being assigned to lipids in the plane and the smallest for those in the toroidal part. The above authors report a temperature span of 10°C to 54°C for which DBBPC/DCPC, $q = 6$, are magnetically oriented. Interestingly, we find even larger temperature ranges (10°C to 75°C) for magnetic alignment. This may be related to the thicker bilayer thickness (C_{14} acyl chains instead of C_{12} for DBBPC) of the TBBPC/DCPC bicelles that could bring more stability to the whole edifice. ^{31}P NMR has also proven to be a nice tool in leading to the construction of temperature-composition and temperature-hydration diagrams of our system. It clearly appears that TBBPC/DCPC systems magnetically orient for 85.7–88.9% TBBPC in the system, for temperatures ranging from 10°C to 75°C at $h = 80\%$, and 84–86% TBBPC content, for temperatures ranging from 10°C to 55°C at $h = 90\%$. The temperature-composition domain where bicelles are magnetically oriented show a pseudoelliptical shape with the wider span in temperature, which points out their high stability with temperature. As a consequence, they can be easily manipulated because they exist at ambient temperature. Surrounding this pure domain, one finds biphasic systems such as oriented disks coexisting with isotropic phases (from the NMR point of view) or systems with cylindrical symmetry (wormlike micelles?); it is clear that these regions are complex and would need further investigation.

Biphenyl versus saturated-chain bicelles

Two important results emerge from the comparative study: 1), bicelle disks are found to be much more stable in temperature, and 2), the trapped water is more ordered. Besides the thermal stability, the temperature-composition domain where TBBPC/DCPC bicelles align with their membrane normal parallel to the magnetic field is very narrow (3%) compared to that of DMPC/DCPC bicelles (22%). This can be accounted for by the small flexibility of the phenyl chain, which allows little adaptation to the perturbation produced by the short-chain lipid DCPC that acts as a detergent. Saturated hydrocarbon chains indeed possess more potential degrees of freedom (*gauche-trans* isomerizations, for instance) to accommodate the strong curvature

promoter made by DCPC. In this respect, DMPC/DCPC bicelles are easier to handle than the TBBPC/DCPC ones; for the latter, small weighing errors in the proportions of the two lipid components will prevent magnetically oriented disk formation. Conversely, the temperature domain of biphenyl-containing species is considerably larger (50°C to 65°C) than that of DMPC/DCPC (10°C to 15°C). This is mainly because of the strong $\Delta\chi$-positive value of the biphenyl moiety, as can be seen with nematic liquid crystal, which also aligns such that the rodlike molecules are parallel to the magnetic field direction. Besides ^{31}P −NMR, which may routinely be used to establish the bicelle diagrams, we have shown that ^{14}N NMR can also be applied on bicelle systems, even if it takes longer (2 h instead of 20 min for ^{31}P NMR) to obtain a very good signal/noise ratio because of the low sensitivity of the nucleus ^{14}N. These experiments nonetheless present a real interest as they provide information about the dynamics of the choline head group. Indeed, because the difference between the ^{14}N quadrupolar splitting of the two types of bicelles results only from their specific average orientation (a factor of ~2), their dynamics can be considered to be very similar. Consequently, the two phenyl rings on one of the TBBPC aliphatic chains little affect the mobility of the head group compared to that of DMPC.

Interestingly, varying hydration in the temperature range where bicelles align in the field leads to similar behavior for the two systems: an increase in hydration yields to a decrease in their orienting capabilities, with the limit reached for 95% water content. A minimum packing (maximum swelling of 95%) is necessary to maintain cooperativity of the objects for keeping their alignment with the magnetic field. The ^{2}H NMR analysis of the deuterated water in orienting biphenyl bicelles shows that ordering properties are more than twice as large as those of saturated-chain analogs. Mainly because of the orientation contribution (factor 2), the water quadrupolar splitting values of the biphenyl bicelles are much higher than those of saturated-chain ones; this presents a real interest for residual dipolar coupling measurements of hydrosoluble peptides or proteins. Moreover, the water in the TBBPC/DCPC system presents ordering properties over a very large temperature range (from 10°C to 70°C), which is another advantage for structural studies of hydrophilic biomolecules. Because of their specific orientation, $n//B_0$, these new bicelles have been shown to be very promising to study hydrophobic peptides also and particularly to determine the orientation of amphipathic peptides using wide-line ^{15}N NMR (37). Nevertheless, the interaction between the two phenyl rings and transmembrane proteins or peptides has to be further investigated.

CONCLUSION

We have succeeded in synthesizing a new phospholipid, TBBPC, which forms magnetically orientable disks when mixed with DCPC, with an average diameter of 800 Å. These disks orient with their normal n parallel to B_0 under specific composition, temperature, and hydration conditions. ^{31}P, ^{14}N, ^{2}H solid-state NMR is a very sensitive technique to map out the domains for magnetic orientation, and SAXS offers a good and original alternative to NMR for characterizing the specific orientation $n//B_0$ of these new bicelles, once they have been annealed in the field. Comparing to the DMPC/DCPC system, TBBPC/DCPC bicelles are much more stable with temperature and offer a very large thermal span for structural studies of either water-dissolved or membrane-embedded proteins.

We gratefully thank Axelle Grelard (UMR 5144 MoBiOS, IECB, Pessac) for her help and her precious advice in NMR spectroscopy, Kathel Bathany (UMR 5144 MoBiOS, IECB, Pessac) for the mass spectrometry analysis, and Franck Artzner (UMR 6626, GMCM, Rennes) for his help in the analysis of SAXS data.

This work was supported by the Centre National de la Recherche Scientifique. We also acknowledge The Aquitaine Region for equipment funding.

REFERENCES

1. Egorova-Zachernyuk, T.A., J. Hollander, N. Fraser, P. Gast, A. J. Hoff, R. Cogdell, H. J. M. de Groot, and M. Baldus. 2001. Heteronuclear 2D-correlations in a uniformly [^{13}C, ^{15}N] labeled membrane-protein complex at ultra-high magnetic fields. *J. Biomol. NMR*. 19:243–253.
2. Marassi, F. M., A. Ramamoorthy, and S. J. Opella. 1997. Complete resolution of the solid-state NMR spectrum of a uniformly ^{15}N-labeled membrane protein in phospholipid bilayers. *Proc. Natl. Acad. Sci. USA*. 94:8551–8556.
3. McDermott, A., T. Polenova, A. Bockmann, K. W. Zilm, E. K. Paulsen, R. W. Martin, and G. T. Montelione. 2000. Partial assignments for uniformly (^{13}C, ^{15}N)-enriched BPTI in the solid state. *J. Biomol. NMR*. 16:209–219.
4. Arora, A., F. Abildgaard, J. H. Bushweller, and L. K. Tamm. 2001. Structure of outer membrane protein A transmembrane domain by NMR spectroscopy. *Nat. Struct. Biol.* 8:334–338.
5. Fernàndez, C., K. Adeishvili, and K. Wüthrich. 2001. Transverse relaxation-optimized NMR spectroscopy with the outer membrane protein OmpX in dihexanoyl phosphatidylcholine micelles. *Proc. Natl. Acad. Sci. USA*. 98:2358–2363.
6. Jones, D. H., K. R. Barber, and C. W. M. Grant. 1998. Sequence-related behaviour of transmembrane domains from class I receptor tyrosine kinases. *Biochim. Biophys. Acta*. 1371:199–212.
7. Da Costa, G., S. Chevance, E. Le Rumeur, and A. Bondon. 2006. Proton NMR detection of porphyrins and cytochrome c in small unilamellar vesicles: role of the dissociation kinetic constant. *Biophys. J*. 90:L55–L57.
8. Sanders, C. R., and K. Oxenoid. 2000. Customizing model membranes and samples for NMR spectroscopic studies of complex membrane proteins. *Biochim. Biophys. Acta*. 1508:129–145.
9. Bechinger, B. 2001. Membrane insertion and orientation of polyalanine peptides: a ^{15}N solid-state NMR spectroscopy investigation. *Biophys. J*. 81:2251–2256.
10. Marassi, F. M., C. Ma, H. Gratkowski, S. K. Straus, K. Sterbel, M. Oblatt-Montal, M. Montal, and S. J. Opella. 1999. Correlation of the structural and functional domains in the membrane protein Vpu from HIV-1. *Proc. Natl. Acad. Sci. USA*. 96:14336–14341.
11. Gabriel, N. E., and M. F. Roberts. 1984. Spontaneous formation of stable unilamellar vesicles. *Biochemistry*. 23:4011–4015.
12. Sanders, C. R., and R. S. Prosser. 1998. Bicelles: a model membrane system for all seasons? *Structure*. 6:1227–1234.
13. Carlotti, C., F. Aussenac, and E. J. Dufourc. 2002. Towards high-resolution ^{1}H-NMR in biological membranes: magic angle spinning of bicelles. *Biochim. Biophys. Acta*. 1564:156–164.
14. Sizun, C., F. Aussenac, A. Grelard, and E. J. Dufourc. 2004. NMR methods for studying the structure and dynamics of oncogenic and

antihistaminic peptides in biomembranes. *Magn. Reson. Chem.* 42:180–186.

15. Arnold, A., T. Labrot, R. Oda, and E. J. Dufourc. 2002. K^+, Na^+, Ca^{2+} and Mg^{2+} modulation of ''bicelle'' size and orientation in a magnetic field as revealed by solid state NMR and electron microscopy. *Biophys. J.* 83:2667–2680.
16. Gaemers, S., and A. Bax. 2001. Morphology of three lyotropic liquid crystalline biological NMR media studied by translational diffusion anisotropy. *J. Am. Chem. Soc.* 123:12343–12352.
17. Nieh, M.-P., C. J. Glinka, S. Krueger, R. S. Prosser, and J. Katsaras. 2001. SANS study of the structural phases of magnetically alignable lanthanide-doped phospholipid mixtures. *Langmuir.* 17:2629–2638.
18. Nieh, M.-P., V. A. Raghunathan, C. J. Glinka, T. A. Harroun, G. Pabst, and J. Katsaras. 2004. Magnetically alignable phase of phospholipid ''bicelle'' mixtures is a chiral nematic made up of wormlike micelles. *Langmuir.* 20:7893–7897.
19. Raffard, G., S. Steinbruckner, A. Arnold, J. H. Davis, and E. J. Dufourc. 2000. Temperature-composition diagram of dimyristoylphosphatidylcholine-dicaproylphosphatidylcholine ''bicelles'' self-orienting in the magnetic field. A solid state ^2H and ^{31}P NMR study. *Langmuir.* 16:7655–7662.
20. Rowe, B. A., and S. L. Neal. 2003. Fluorescence probe study of bicelle structure as a function of temperature: developing a practical bicelle structure model. *Langmuir.* 19:2039–2048.
21. Soong, R., and P. M. Macdonald. 2005. Influence of the long-chain/short-chain amphiphile ratio on lateral diffusion of PEG-lipid in magnetically aligned lipid bilayers as measured via pulsed-field-gradient NMR. *Biophys. J.* 88:255–268.
22. van Dam, L., G. Karlsson, and K. Edwards. 2004. Direct observation and characterization of DMPC/DHPC aggregates under conditions relevant for biological solution NMR. *Biochim. Biophys. Acta.* 1664:241–256.
23. Bax, A., and N. Tjandra. 1997. High-resolution heteronuclear NMR of human ubiquitin in an aqueous liquid crystalline medium. *J. Biomol. NMR.* 10:289–292.
24. Lancelot, N., K. Elbayed, and M. Piotto. 2005. Applications of variable-angle sample spinning experiments to the measurement of scaled residual dipolar couplings and ^{15}N CSA in soluble proteins. *J. Biomol. NMR.* 37:153–161.
25. Tjandra, N., and A. Bax. 1997. Direct measurement of distances and angles in biomolecules by NMR in a dilute liquid crystalline medium. *Science.* 278:1111–1114.
26. Zandomeneghi, G., M. Tomaselli, J. D. Beek, and B. H. Meier. 2001. Manipulation of the director in bicellar mesophases by sample spinning: a new tool for NMR spectroscopy. *J. Am. Chem. Soc.* 123:910–913.
27. Katsaras, J., R. L. Donaberger, J. P. Swainson, D. C. Tennant, Z. Tun, R. R. Vold, and R. S. Prosser. 1997. Rarely observed phase transitions in a novel lyotropic liquid crystal system. *Phys. Rev. Lett.* 78:899–902.
28. Prosser, R. S., H. Bryant, R. G. Bryant, and R. R. Vold. 1999. Lanthanide chelates as bilayer alignment tools in NMR studies of membrane-associated peptides. *J. Magn. Reson.* 141:256–260.
29. Prosser, R. S., J. A. Hunt, J. A. Dinatale, and R. R. Vold. 1996. Magnetically aligned membrane model systems with positive order parameters: switching the sign of S_{zz} with paramagnetic ions. *J. Am. Chem. Soc.* 118:269–270.
30. Prosser, R. S., J. S. Hwang, and R. R. Vold. 1998. Magnetically aligned phospholipids bilayers with positive ordering: a new model membrane system. *Biophys. J.* 74:2405–2418.
31. Picard, F., M. J. Paquet, J. Levesque, A. Bélanger, and M. Auger. 1999. ^{31}P NMR first spectral moment study of the partial magnetic orientation of phospholipid membranes. *Biophys. J.* 77:888–902.
32. Sanders, C. R., J. E. Schaff, and J. H. Prestegard. 1993. Orientational behavior of phosphatidylcholine bilayers in the presence of aromatic amphiphiles and a magnetic field. *Biophys. J.* 64:1069–1080.
33. Sakurai, I., Y. Kawamura, A. Ikegami, and S. Iwayanagi. 1980. Magneto-orientation of lecithin crystals. *Proc. Natl. Acad. Sci. USA.* 77:7232–7236.
34. Visscher, I., M. C. A. Stuart, and J. B. F. N. Engberts. 2006. The influence of phenyl and phenoxy modification in the hydraophobic tails of di-*n*-alkyl phosphate amphiphiles on aggregate morphology. *Org. Biomol. Chem.* 4:707–712.
35. Cho, G., B. M. Fung, and V. B. Reddy. 2001. Phospholipid bicelles with positive anisotropy of the magnetic susceptibility. *J. Am. Chem. Soc.* 123:1537–1538.
36. Tan, C., B. M. Fung, and G. Cho. 2002. Phospholipid bicelles that align with their normals parallel to the magnetic field. *J. Am. Chem. Soc.* 124:11827–11832.
37. Loudet, C., L. Khemtemourian, F. Aussenac, S. Gineste, M. F. Achard, and E. J. Dufourc. 2005. Bicelle membranes and their use for hydrophobic peptide studies by circular dichroism and solid state NMR. *Biochim. Biophys. Acta.* 1724:315–323.
38. Rance, M., and R. A. Byrd. 1983. Obtaining high-fidelity spin-1/2 powder spectra in anisotropic media: phase-cycled Hahn echo spectroscopy. *J. Magn. Reson.* 52:221–240.
39. Davis, J. H. 1979. Deuterium magnetic resonance study of the gel and liquid crystalline phases of dipalmitoylphosphatidylcholine. *Biophys. J.* 27:339–358.
40. Charvolin, J., P. Mannevill, and B. Deloche. 1975. Magnetic resonance of perdeuterated potassium laurate in oriented soap-water multilayers. *Chem. Phys. Lett.* 23:345–348.
41. Seelig, J. 1977. Deuterium magnetic resonance: theory and application to lipid membranes. *Q. Rev. Biophys.* 10:353–418.
42. Pott, T., and E. J. Dufourc. 1995. Action of melittin on the DPPC-cholesterol liquid-ordered phase: a solid state ^2H and ^{31}P-NMR study. *Biophys. J.* 68:965–977.
43. Aussenac, F., B. Lavigne, and E. J. Dufourc. 2005. Towards bicelle stability with ether-linked phospholipids: temperature, composition and hydration diagrams by ^2H and ^{31}P solid state NMR. *Langmuir.* 21:7129–7135.
44. Perly, B., E. J. Dufourc, and H. C. Jarrell. 1984. Facile and high yielding synthesis of phosphatidylcholines and phosphatidylethanolamines containing ^2H-labeled acyl chains. *J. Labelled Compd. Radiopharm.* 21: 1–13.
45. Bolze, J., T. Fujisawa, T. Nagao, K. Norisada, H. Saitô, and A. Naito. 2000. Small angle x-ray scattering and ^{31}P NMR studies on the phase behavior of phospholipid bilayered mixed micelles. *Chem. Phys. Lett.* 329:215–220.
46. Etrillard, J., M. A. V. Axelos, I. Cantat, F. Artzner, A. Renault, T. Weiss, R. Delannay, and F. Boué. 2005. In situ investigations on organic foam films using neutron and synchrotron radiation. *Langmuir.* 21:2229–2234.
47. Lamy-Freund, M. T., and K. A. Riske. 2003. The peculiar thermo-structural behavior of the anionic lipid DMPG. *Chem. Phys. Lipids.* 122:19–32.
48. Riske, K. A., L. Q. Amaral, and M. T. Lamy-Freund. 2001. Thermal transitions of DMPG bilayers in aqueous solution: SAXS structural studies. *Biochim. Biophys. Acta.* 1511:297–308.
49. Davis, J. H. 1983. The description of membrane lipid conformation, order and dynamics by ^2H-NMR. *Biochim. Biophys. Acta.* 737:117–171.
50. Douliez, J.-P., A. Léonard, and E. J. Dufourc. 1996. Conformational order of DMPC *sn*-1 versus *sn*-2 chains and membrane thickness: an approach to molecular protrusion by solid state ^2H-NMR and neutron diffraction. *J. Phys. Chem.* 100:18450–18457.
51. Léonard, A., C. Escrive, M. Laguerre, E. Pebay-Peyroula, W. Néri, T. Pott, J. Katsaras, and E. J. Dufourc. 2001. Location of cholesterol in DMPC membranes. A comparative study by neutron diffraction and molecular mechanics simulation. *Langmuir.* 17:2019–2030.
52. Léonard, A., J.-C. Maillet, J. Dufourcq, and E. J. Dufourc. 1992. Bilayer thickness from lipid-chain dynamics: influence of cholesterol and electric charges. A ^2H-NMR approach. *Prog. Colloid Polym. Sci.* 89:315–318.
53. Katsaras, J., R. L. Donaberger, D. C. Swainson, Z. Tun, R. R. Vold, and R. S. Prosser. 1997. Rarely observed phase transitions in a novel lyotropic liquid crystal system. *Phys. Rev. Lett.* 78:899–902.